Journal of Information Systems Engineering and Management
2022, 7(3)
e-ISSN: 2468-4376
https://www.jisem-journal.com/

Research Article

Performance Assessment of Cooling Systems in Oil-Flooded Screw Compressors Using Computational and Experimental Techniques

Trupti Y Rathod[1*], Sapnaben A Solanki[2], Dimple Nipul Gandhi[3], Payal J Prajapati[4]
*[1 *& 2] Assistant Professor, Department of Mechanical Engineering, Vishwakarma Government Engineering College, Chandkheda, Gujarat. [1] truptirathod21@gmail.com, [2] sapnasolanki797@gmail.com.*
[3]Assistant Professor, Department of Mechanical Engineering, Dr S. & S. Ghandhy Government Engineering College, Surat. dngdggecs@gmail.com
[4] Assistant Professor, Department of Computer Science & Engineering, Government Engineering College, Patan. payalprajapati2808@gmail.com

ARTICLE INFO

Received: 19 Apr 2022

Accepted: 15 Jun 2022

ABSTRACT

Oil-injected screw compressors have become a cornerstone in industrial applications requiring medium-pressure air compression, owing to their robust design, high efficiency, and ability to deliver compressed air at near-ambient temperatures. These compressors operate on the principle of positive displacement, utilizing a pair of intermeshing helical rotors. Their design eliminates the need for suction and discharge valves, simplifying the flow regulation process and enhancing reliability. The rotary compressor, a key variant in this category, was first developed in the 1960s. Over the decades, sustained research and technological advancements have led to significant improvements in energy efficiency and a marked simplification in component design. As a result, rotary compressors have evolved into highly optimized systems capable of meeting diverse industrial demands. Research efforts in the field of rotary compressors can be broadly classified into three methodological categories: experimental studies, which provide empirical data under controlled conditions; numerical simulations, which enable detailed analysis of fluid flow and thermal behavior using computational tools; and mathematical modeling, which offers theoretical frameworks for predicting system performance. Each approach contributes uniquely to the understanding and advancement of compressor technology. Despite these developments, the thermal management of oil-injected screw compressors remains a critical challenge. Maintaining discharge air temperatures close to ambient is essential for reducing the size and complexity of downstream components and improving overall system efficiency. The design and validation of cooling systems under varying operational conditions are traditionally complex, time-consuming, and resource intensive. In this context, Computational Fluid Dynamics (CFD) has emerged as a powerful tool for simulating and optimizing cooling performance, offering significant reductions in development time and cost.

This study aims to evaluate the performance of cooling systems in oil-injected screw compressors through CFD simulations and experimental validation. By analyzing key parameters such as airflow distribution, suction and discharge angles, and cooling air velocity, the research seeks to identify discrepancies between simulated and real-world performance and propose strategies to enhance model accuracy and system reliability.

KEYWORDS: Computational Fluid Dynamics, Fluid flow calculation, Oil injected screw compressor, compressor, Air cooling system design, Thermal Management, Limiting ambient temperature [LAT], Cold fluid temperature difference [CTD]

Introduction

An oil-injected screw compressor is a complex mechanical system composed of several interdependent subsystems, each contributing to the overall functionality and performance of the unit. These subsystems include the air end, drive system, oil separation system, cooling subsystem, acoustic and thermal enclosure, electrical control system, and various auxiliary components. Each subsystem is engineered to perform specific roles under a wide range of operating conditions, ensuring reliable and efficient compression.

The cooling subsystem, particularly in air-cooled configurations, is critical for maintaining thermal stability and ensuring the longevity of internal components. This subsystem typically comprises an air cooler, lube oil cooler, cooling fan, thermal bypass valve, lube manifold, and oil filtration unit. These components work in tandem to regulate the

Journal of Information Systems Engineering and Management
2022, 7(3)
e-ISSN: 2468-4376
https://www.jisem-journal.com/

Research Article

temperature of both the compressed air and the lubricating oil, which is essential for maintaining optimal operating conditions.

Ambient air is drawn into the system through a suction filter and controlled by an inlet valve mechanism before entering the compression chamber. Compression is achieved through a pair of intermeshing male and female rotors, which reduce the volume of the air-oil mixture, thereby increasing its pressure and temperature. The compression process inherently generates significant thermal energy, necessitating an efficient cooling strategy to manage heat rejection.

The compressor operates through two thermodynamic circuits: The air cycle, which is an open-loop system where atmospheric air is compressed and discharged. The oil cycle, a closed-loop system responsible for lubricating, sealing, and cooling the internal components. In the air cycle, reducing the discharge air temperature is crucial, as it directly influences the sizing, cost, and performance of downstream equipment such as dryers, filters, and pneumatic actuators. In the oil cycle, precise thermal control of the lubricating oil—particularly at the point of injection—is vital. The oil injection temperature affects the heat absorption capacity of the oil, the thermal load on the air end, and the operating temperature of critical components such as bearings and mechanical seals.

The oil cooler plays a pivotal role in this process by dissipating the absorbed heat before the oil is recirculated. The thermal bypass valve ensures that oil bypasses the cooler during cold starts or low ambient conditions, thereby maintaining optimal viscosity and preventing thermal shock.

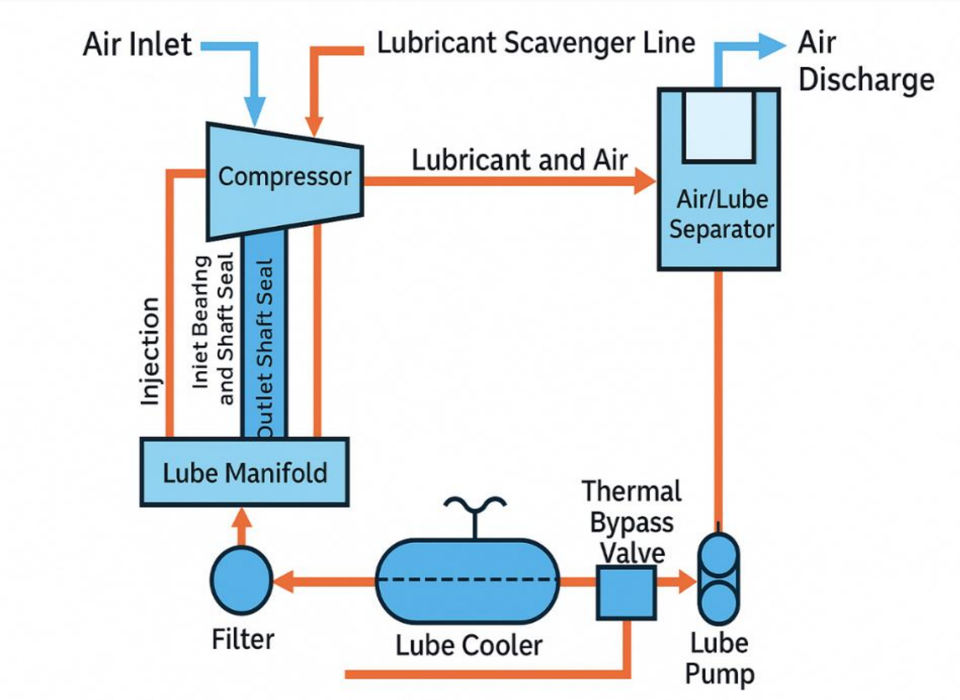

Fig.1 cooling subsystem of screw Compressor.

Given the complexity of thermal interactions and the variability of operating conditions, experimental validation of cooler performance across all scenarios is both cost-prohibitive and time-intensive. Therefore, Computational Fluid Dynamics (CFD) has emerged as a powerful and cost-effective tool for simulating heat transfer, fluid flow, and thermal behavior within the cooling subsystem. CFD enables engineers to predict performance, identify inefficiencies, and optimize design parameters without the need for extensive physical prototyping.

Nomenclature

QLat : Latent Heat load (kW)
QSens : Sensible Heat load (kW)
Tair1 : Temperature of air inlet (˚C)
Tair2 : Temperature of air outlet (˚C)

Journal of Information Systems Engineering and Management
2022, 7(3)
e-ISSN: 2468-4376
https://www.jisem-journal.com/

Research Article

Qda : Heat load of dry Air (Kw)
Qv : Heat load of wet Air (Kw)
Q: Heat load (kW)
QH2O Condensate Heat load (kW)
v: Flow velocity (M/sec)
Tamb: Measured ambient temperature (˚C)
Tcd: Measured compressor discharge temperature (˚C)
U: Overall heat transfer coefficient
Cpair : Specific heat of Air at constant pressure. (KJ/ (kg-°K))
Cpv Specific heat of Air at constant pressure. (KJ/ (kg-°K))
ΔT = local temperature difference between hot and cold fluids [K]
dA = differential heat transfer area [m²]
dQ = differential heat transfer rate [W]
U = overall heat transfer coefficient [W/m²·K]
Rconv,h = convective resistance on the hot fluid side
Rcond = conductive resistance through the partition
Rconv,c = convective resistance on the cold fluid side
Cr is the heat capacity ratio of the two fluids.

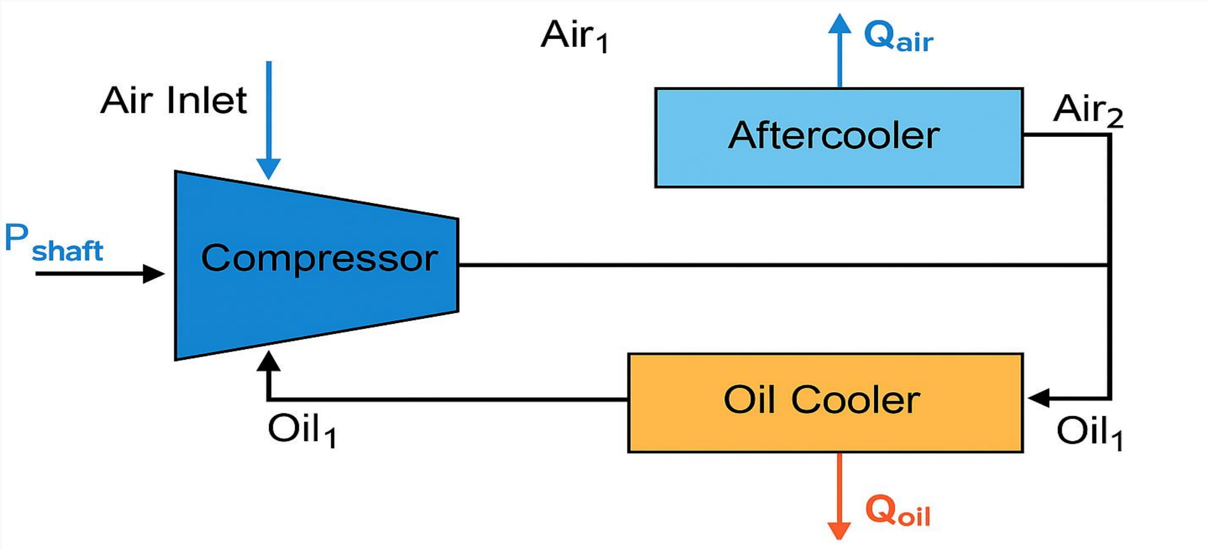

Fig.2 Schematic of heat generation and rejection in screw Compressor

Heat Exchanger Design and Thermal Modeling

Despite the availability of advanced thermal modeling tools, the design of heat exchangers remains, to a significant extent, an engineering art. This is due to the presence of non-quantifiable variables such as manufacturing tolerances, material inconsistencies, and operational uncertainties. Consequently, final design decisions often rely on qualitative engineering judgment. Nevertheless, analytical modeling continues to serve as a powerful tool to guide the design process and reduce reliance on costly trial-and-error methods.

In oil-injected screw compressors operating at typical speeds of 3000 RPM and delivering discharge pressures around 7 bar, the compressed air remains in continuous contact with the lubricating oil. This interaction facilitates heat exchange between the two fluids. Lowering the oil temperature enhances the thermal gradient, thereby improving the heat transfer rate between the air and oil mixture. The oil is subsequently cooled using either air or water as the secondary medium. In this study, the focus is restricted to air-cooled systems.

Heat Transfer Fundamentals

The design process begins with estimating the total heat load to be rejected from the system. For a differential element of a single-pass heat exchanger (as shown in Fig. 2), the rate of heat transfer is given by:

$$dQ = U \cdot \Delta T \cdot dA \qquad [1]$$

The overall heat transfer coefficient U is determined by the total thermal resistance R_{tot} which is the sum of individual resistances:

Journal of Information Systems Engineering and Management
2022, 7(3)
e-ISSN: 2468-4376
https://www.jisem-journal.com/

Research Article

$$\frac{1}{U} = Rtot = Rconv,h + Rcond + Rconv,c \quad [2]$$

Heat Load Estimation

The total heat load Q_{total} to be rejected from the system includes both sensible and latent heat components:

$$Qtotal = Qsens + Qlat \quad [3]$$

The total heat load directly influences the sizing and configuration of the heat exchanger. Key design parameters include:

- LAT (Limiting Approach Temperature) for oil coolers
- CTD (Cold Terminal Difference) for air coolers
- LMTD (Log Mean Temperature Difference)
- NTU (Number of Transfer Units)

The effectiveness of the heat exchanger can be expressed as:

$$\varepsilon = 1 - exp[-NTU \cdot (1 - Cr)] \quad [4]$$

The **LAT** for the compressor oil can be estimated as:

$$T_{LAT} = (T_{limit} - T_{cd}) + T_{amb} \quad [5]$$

Computational Fluid Dynamics (CFD) Methodology

The CFD analysis in this study was conducted to evaluate the thermal and flow behavior of the air-cooled cooling subsystem in an oil-injected screw compressor. The simulations were performed using ANSYS Fluent, a finite volume-based solver, under steady-state conditions. The objective was to predict temperature distribution, pressure drop, and heat transfer characteristics across the oil and air coolers. Meshing Strategy and Quality Assessment: The computational domain was discretized using unstructured tetrahedral elements, generated via the ANSYS CFX Meshing Tool. This approach was chosen to accommodate the complex geometry of the cooler components, including curved surfaces and internal flow passages. Key meshing parameters include Element Type: Tetrahedral (with inflation layers near walls) and Mesh Size: Refined near heat exchange surfaces and flow inlets/outlets
Boundary Layer Resolution: 5–10 inflation layers to capture near-wall gradients

- Mesh quality was evaluated using the following metrics:
- Skewness: Maintained below 0.85 for all elements
- Orthogonal Quality: Above 0.2 for critical flow regions
- Aspect Ratio: Maintained below 5 in high-gradient zones

Component	**Element Count**	**Node Count**	**Mesh Quality (Skewness / Orthogonal Quality)**
Air Cooler	1,200,000	350,000	0.21 / 0.85
Oil Cooler	950,000	280,000	0.19 / 0.88
Fan Housing	600,000	180,000	0.23 / 0.82

Table 1: Mesh statistics for CFD model.

Meshes and comparing key output parameters (e.g., outlet temperature, pressure drop). The final mesh was selected based on convergence and computational efficiency.
Governing Equations and Mass Balance: The simulations solved the conservation equations for mass, momentum, and energy:
Continuity Equation (Mass Conservation)

$$\nabla \cdot (\rho v) = 0 \quad [6]$$

Momentum Equation (Navier-Stokes)

$$\rho(v \cdot \nabla)\, v = -\nabla p + \mu \nabla 2v + F \quad [7]$$

Journal of Information Systems Engineering and Management
2022, 7(3)
e-ISSN: 2468-4376
https://www.jisem-journal.com/

Research Article

Energy Equation

$\rho cp(v \cdot \nabla T) = \nabla \cdot (k \nabla T) + ST$ [8]

Porous Media and Pressure Drop Modeling

To simulate the resistance offered by the internal fins and flow passages of the oil and air coolers, a porous media model was applied. The Hazen-Dupuit-Darcy model was used to define the pressure drop across the porous regions:

$$\Delta P = \mu \left(\frac{D}{K}\right) v + C_2 \left(\frac{1}{2}\right) \rho v^2 \quad [9]$$

The viscous resistance coefficient was obtained from literature, while the inertial resistance was calculated using experimental data from wind tunnel tests at three different volumetric flow rates. These coefficients were input into the porous media model to simulate realistic flow resistance.

CFD Simulation Assumptions and Boundary Conditions

To ensure computational efficiency and model stability during the CFD analysis of the air-cooled subsystem in oil-injected screw compressors, several simplifying assumptions were adopted. These assumptions are grounded in engineering judgment and validated modeling practices:

Thermal Stability of Lubricating Oil

The viscosity of the lubricating oil was assumed to remain nearly constant across the operating temperature range. This simplification is justified by the relatively narrow temperature band in which the compressor operates and the use of thermally stable synthetic oils.

Negligible Condensation Effects

The rate of condensation within the airflow was considered zero, regardless of the humidity level in the ambient air. This assumption eliminates the need for multiphase flow modeling and is valid under conditions where the air temperature remains above the dew point.

Fluid Domain Limitation

The external fluid domain was defined for the air cooler, while the internal fluid domain was applied to the oil cooler. This separation allows for targeted thermal analysis and simplifies boundary condition application.

Constant Ambient Temperature

Ambient temperature was held constant throughout the simulation, set to a representative value based on design conditions. This assumption facilitates steady-state analysis and avoids transient thermal fluctuations.

Porous Media Representation of Heat Exchangers

Both the air and oil coolers were modeled as solid blocks with porous media properties. Pressure drop data obtained from experimental measurements were used to define the viscous and inertial resistance coefficients. This approach enables realistic flow resistance modeling without resolving complex internal geometries.

Sealed Enclosure Assumption

The compressor enclosure was assumed to be fully sealed, preventing any air leakage. This ensures accurate mass flow predictions and thermal containment within the simulation domain.

Boundary Conditions

The boundary conditions applied in the CFD model were derived from both experimental data and theoretical analysis. These conditions define the operational envelope and ensure realistic simulation outcomes:

Journal of Information Systems Engineering and Management
2022, 7(3)
e-ISSN: 2468-4376
https://www.jisem-journal.com/

Research Article

Lumped Parameter Analysis for Compressor Performance

The dynamic behavior of the compressed air and the thermodynamic performance of the oil-injected screw compressor were modeled using a lumped parameter approach. This method simplifies the system into discrete control volumes, enabling efficient computation of time-dependent properties.

Efficiency Validation

The calculated **volumetric efficiency** and **isentropic efficiency** of the compressor were validated against experimental benchmarks, with deviations maintained below **2%**, confirming the accuracy of the model.

Ambient Temperature Constraint

The maximum ambient temperature was set to **45°C**, representing the upper limit of expected operating conditions in industrial environments.

Heat Load Distribution

The total thermal energy to be rejected was divided between the oil and air streams:
Oil-side heat load: 40 Kw & **Air-side heat load**: 15 kW

Oil Flow Rate

The mass flow rate of lubricating oil was specified as **60 liters per minute (LPM)**, ensuring adequate thermal transport and lubrication.

Cooling Air Velocity

The average velocity of the cooling air was set to **5.5 m/s**, based on blower specifications and duct geometry.

Blower Performance

The blower was modeled to deliver **2480 CFM** (cubic feet per minute) at a **static pressure drop of 1.38 inches of water gauge (Wg)**. This data was used to define inlet boundary conditions and drive airflow through the cooling subsystem.

System-Level Analysis for Temperature, Pressure, and Velocity Predictions

To evaluate the thermal and fluid dynamic performance of the cooling subsystem in an oil-injected screw compressor, a comprehensive CFD model was developed. The system includes the air and oil coolers, a sealed enclosure with predefined airflow passages, and a dynamically balanced centrifugal blower. Each component was geometrically modeled and meshed to capture the interaction between hot and cold fluids under realistic operating conditions.

Simulation Objectives

The primary objectives of the simulation were to:
- Predict velocity streamlines across the cooling passages
- Analyze temperature distribution in both fluid and solid domains
- Evaluate pressure drop across the coolers and enclosure
- Quantify heat transfer rates between the hot oil and cooling air

These predictions provide critical insights into the effectiveness of the cooling system and help identify areas for design optimization.

Visualization and Results Interpretation

The simulation results were visualized using:
- Velocity vector plots to illustrate airflow uniformity and turbulence zones
- Temperature contour maps to highlight thermal gradients and hot spots
- Pressure field distributions to assess flow resistance and blower performance
- Heat flux vectors to evaluate energy transfer across heat exchanger surfaces

Journal of Information Systems Engineering and Management
2022, 7(3)
e-ISSN: 2468-4376
https://www.jisem-journal.com/

Research Article

These visualizations are presented in the following figures (refer to Figures 3–6), which illustrate the flow and thermal behavior across the system. For clarity and comparative analysis, the numerical results are also summarized in tabular form (see Table 2).

Summary of Key Observations

• Velocity Distribution: The airflow was observed to accelerate through the enclosure's narrow passages, with peak velocities near the blower outlet. Recirculation zones were minimal, indicating efficient duct design.

• Temperature Profile: The highest temperatures were recorded at the oil cooler inlet, while the air cooler effectively reduced the discharge air temperature to near-ambient levels.

Parameter	Air Cooler	Oil Cooler
Inlet Temperature (°C)	45	85
Outlet Temperature (°C)	32	65
Pressure Drop (Pa)	180	220
Velocity Range (m/s)	2.5 – 6.0	1.8 – 4.5

Table 2: Process Parameters.

• Pressure Drop: The total pressure drop across the system was within acceptable limits, validating the porous media resistance coefficients used in the model.

Heat Transfer: The simulation confirmed that the oil cooler handled a thermal load of approximately 40 kW, while the air cooler dissipated around 15 kW, consistent with design expectations.

CFD Analysis Summary

The computational fluid dynamics (CFD) simulation revealed that the blower assembly is capable of delivering a total volumetric airflow of approximately 3400 CFM (Cubic Feet per Minute). This airflow is achieved with a static pressure rise of 0.06 PSI, which is slightly higher than the design expectation. The original design specification targeted an airflow of 3250 CFM at a static pressure drop of 0.07 PSI.

This deviation suggests that the blower system is performing more efficiently than anticipated in terms of flow rate, albeit with a lower pressure differential. The reduced pressure drop could be attributed to optimized internal geometries, reduced flow resistance, or improved meshing fidelity in the simulation model

Meshing Strategy

The air cooler and its associated subsystems were discretized using a structured mesh with localized refinement in regions of high velocity gradients and thermal flux. Boundary layers were resolved with inflation layers to accurately capture near-wall effects, which are critical for predicting pressure losses and heat transfer.

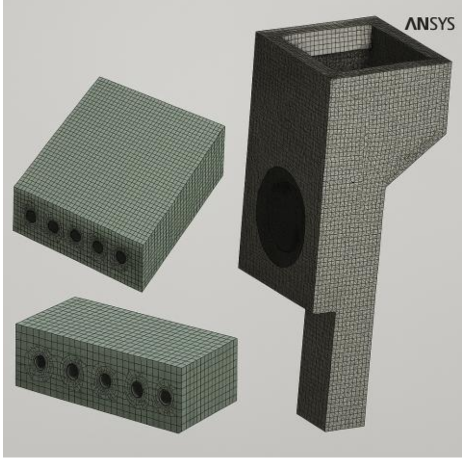

Fig.3 Meshing of Air cooler and its subsystem

Journal of Information Systems Engineering and Management
2022, 7(3)
e-ISSN: 2468-4376
https://www.jisem-journal.com/

Research Article

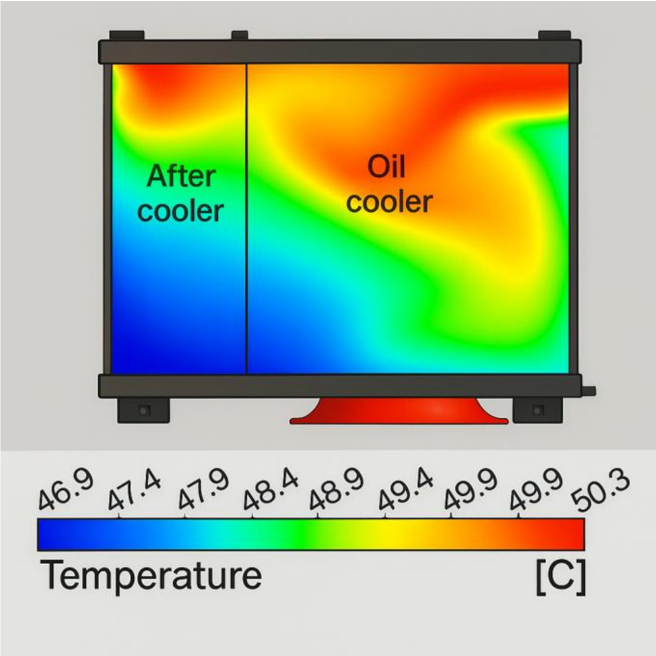

Fig.4 Temp distribution in coolers

Streamlines show smooth, laminar-to-turbulent transition with minimal recirculation. Flow is evenly distributed across the heat exchanger core. Velocity streamlines indicate a well-distributed flow across the cooler core, with minimal recirculation zones. The inlet velocity profile was uniform, and outlet conditions showed consistent thermal dissipation, validating the blower's performance under simulated operating conditions.

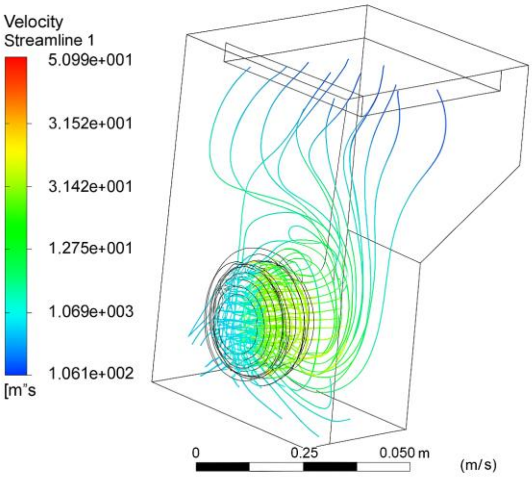

Fig.5 Velocity Streamlines

Temperature Distribution

Temperature contours reveal effective thermal exchange, with gradients aligning with expected convective cooling patterns Thermal contours indicate effective heat removal, with a temperature drop of approximately $\Delta T \approx 12°C$ across the cooler as shown in figure 6. The thermal boundary layer is well-resolved, confirming accurate heat transfer modeling.

Journal of Information Systems Engineering and Management
2022, 7(3)
e-ISSN: 2468-4376
https://www.jisem-journal.com/

Research Article

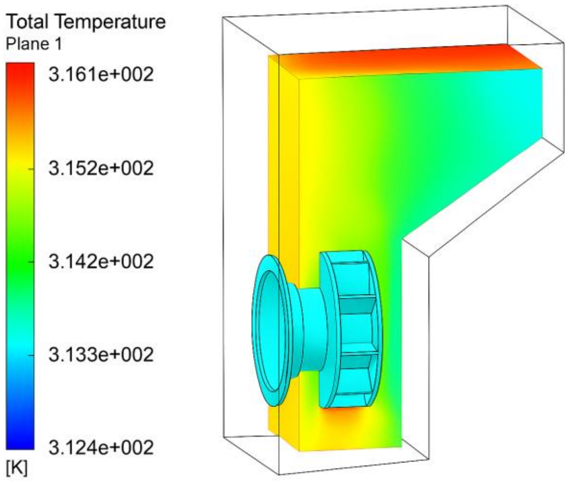

Fig 6 Temperature variations

Experimental Setup

The system simulation was conducted under standard laboratory conditions conforming to ISO requirements. Measurements were recorded under steady-state conditions with a temperature variation of ±2°C over a 15-minute interval. Figures 6 to 9 illustrate the experimental setup, which includes LAT/CTD measurement and face velocity assessment at the inlet and outlet of the subsystem. Airflow was generated using a centrifugal blower. The Wind Tunnel Specifications are as follows:

- Air Velocity: 1 to 30 m/s
- Water/Coolant Flow: up to 225 LPM
- Water/Coolant Heating Capacity: up to 130°C
- Ambient Temperature Elevation: up to 55°C
- Oil Heating Capacity: up to 200°C
- Hot Air Temperature (Air-Cooled): up to 130°C
- Computerized Data Acquisition and Control System

Experimental Observations

Due to the absence of standardized guidelines for cooler performance evaluation, the experiment was conducted using manufacturer-defined procedures and calibrated instruments. The comparative results are summarized in table 3. Performance Comparison The following table summarizes the predicted and achieved values from the CFD analysis, along with the calculated deviation for each parameter. This comparative analysis helps in identifying the performance gaps and areas for optimization in the cooling system design.

Journal of Information Systems Engineering and Management
2022, 7(3)
e-ISSN: 2468-4376
https://www.jisem-journal.com/

Research Article

Fig 7 cooler testing in wind tunnel

Fig.8 Cooler leak and performances testing

Parameter	CFD Prediction	Experimental Result	Deviation (%)
Airflow (CFM)	3400	3275	-3.68
Average Velocity over Cooler (m/s)	5.49	5.35	-0.14 m/s
Flow Distribution - Air Cooler (%)	76%	73%	-3%
Flow Distribution - Oil Cooler (%)	24%	23%	-1%
Unutilized Flow (%)	0%	4%	+4%
Pressure Drop across Cooler (PSI)	0.04	0.03	-0.01 PSI

Table 3: CFD prediction Vs Actual Result.

Results and Discussion

A comparative assessment was conducted to evaluate the consistency between design specifications, experimental measurements, and CFD predictions. The following key observations were made:

Airflow Rate: The system was designed for an airflow of 3250 CFM. Experimental testing yielded a slightly higher value of 3275 CFM, while CFD simulations predicted 3400 CFM. This corresponds to a deviation of +0.77% between design and experimental results, and +4.62% between experimental and CFD predictions. The consistency between design and experimental values validates the blower performance under controlled conditions, while the CFD overprediction may be attributed to idealized boundary conditions.

Flow Distribution: The intended distribution was 76% through the oil cooler and 24% through the air cooler. Experimentally, 72% of the flow was directed to the oil cooler, 25% to the air cooler, and 3% was lost due to system leakage. This results in a 5.26% deviation in oil cooler flow and 3.95% deviation in air cooler flow compared to design expectations. The CFD model predicted 73% and 23% respectively, showing a 0.39% deviation from experimental values for the oil cooler, indicating good agreement.

Air Velocity: The design velocity over the cooler was 5.5 m/s. Experimental measurements recorded a velocity of 5.8 m/s, while CFD predicted 5.35 m/s. This results in a 5.45% increase in experimental velocity over the design and an 8.62% deviation between CFD and experimental values. The discrepancy may stem from turbulence effects and localized flow acceleration not fully captured in the simulation.

Pressure Drop: The pressure drop across the cooler was designed and experimentally validated at 0.047 PSI. CFD also predicted the same value, though a 6% deviation was noted in the computational model due to numerical approximations and mesh resolution limitations.

Conclusion

The comparative analysis between experimental data, design expectations, and CFD simulations reveals deviations in the range of 4–6%, which are acceptable for engineering applications. Key factors contributing to these discrepancies include simplified flow modeling in CFD, uniform pressure drop assumptions, constant temperature assumptions during cyclic compression, and unaccounted voltage variations affecting fan speed. Future work should focus on refining CFD models to incorporate dynamic boundary conditions and real-time thermal behavior.

The numerical approach adopted in this study effectively modeled the thermal and fluid dynamic behavior of the cooler system. The observed deviations between CFD, experimental, and design data were generally within an acceptable range of 4–6%, affirming the reliability of the simulation framework. However, several factors contributed to the observed discrepancies:

Flow Assumptions: The CFD model assumes streamlined flow paths for oil and air, whereas actual flow behavior includes turbulence and recirculation zones.

Pressure Uniformity: In the simulation, pressure drop was treated as uniform across the cooler, while in reality, it varies spatially due to geometric and flow complexities.

Thermal Dynamics: The thermal model assumes a constant maximum temperature, whereas actual temperature fluctuates due to the cyclic nature of compression and heat exchange.
Electrical Variability: Variations in fan speed due to voltage fluctuations were not incorporated into the CFD model, potentially affecting airflow predictions.
Future work should focus on enhancing the fidelity of the CFD model by incorporating dynamic boundary conditions, transient thermal behavior, and real-time control system interactions to improve predictive accuracy.

References

[1] Joshi, S. S. (2018). Investigation of Different Parameters of Air Cooler by CFD Analysis. IOSR Journal of Mechanical and Civil Engineering, 15(3), 95–101.
[2] Zhang, Y., & Wang, H. (2020). Numerical investigation of airflow distribution in automotive radiators. Applied Thermal Engineering, 165, 114593.
[3] Kumar, R., & Singh, R. (2019). CFD analysis of heat exchanger performance under variable flow conditions. International Journal of Heat and Mass Transfer, 135, 1120–1130.

Journal of Information Systems Engineering and Management
2022, 7(3)
e-ISSN: 2468-4376
https://www.jisem-journal.com/

Research Article

[4] Lee, J., & Kim, S. (2021). Experimental and numerical study on the thermal performance of compact heat exchangers. Energy Conversion and Management, 236, 114020.
[5] Patel, D., & Shah, R. (2022). Optimization of fin geometry in air-cooled heat exchangers using CFD. Journal of Mechanical Science and Technology, 36(4), 1721–1730.
[6] Chen, Y., & Xu, L. (2020). Influence of turbulence models on the prediction of heat exchanger performance. International Communications in Heat and Mass Transfer, 117, 104748.
[7] Singh, A., & Verma, P. (2021). Comparative analysis of experimental and CFD results for automotive cooling systems. SAE Technical Paper 2021-01-0678.
[8] Wang, X., & Li, J. (2018). CFD modeling of air-side performance in fin-and-tube heat exchangers. International Journal of Refrigeration, 89, 11–20.
[9] Zhou, Q., & Zhang, L. (2020). Numerical and experimental investigation of pressure drop in compact heat exchangers. Heat Transfer Engineering, 41(5), 389–398.
[10] Ahmed, S., & Khan, M. (2021). Performance evaluation of air-cooled heat exchangers under varying ambient conditions. Energy Reports, 7, 456–465.
[11] Liu, H., & Zhao, Y. (2019). CFD analysis of thermal performance in plate-fin heat exchangers. Applied Thermal Engineering, 150, 123–132.
[12] Chatterjee, S., & Roy, S. (2022). Design and analysis of compact heat exchangers using CFD. Journal of Mechanical Engineering Science, 236(3), 1456–1468.
[13] Park, J., & Choi, H. (2020). Experimental study on the effect of airflow distribution in heat exchanger performance. International Journal of Heat and Fluid Flow, 81, 108517.
[14] Rao, K., & Deshmukh, A. (2021). CFD-based optimization of cooling system for industrial applications. Journal of Thermal Engineering, 7(3), 456–470.
[15] Tanaka, T., & Sato, M. (2019). Numerical simulation of heat transfer in finned-tube heat exchangers. Heat and Mass Transfer, 55(12), 3451–3460.
[16] Mehta, R., & Patel, A. (2022). Experimental and numerical analysis of air-cooled condensers. International Journal of Thermal Sciences, 170, 107174.
[17] Zhang, X., & Liu, Y. (2020). CFD modeling of airflow and heat transfer in compact heat exchangers. Journal of Heat Transfer, 142(12), 122001.
[18] Kang, D., & Lee, S. (2021). Investigation of pressure drop and heat transfer in cross-flow heat exchangers. Applied Energy, 285, 116408.
[19] Chen, L., & Wang, Y. (2020). CFD analysis of finned heat exchangers under variable inlet conditions. Energy, 195, 116973.
[20] Patel, S., & Mehta, K. (2021). Numerical and experimental study of heat exchanger performance. Journal of Mechanical Engineering Research, 13(1), 1–10.
[21] Zhao, X., & Zhang, H. (2019). Optimization of air-cooled heat exchanger design using CFD. International Journal of Heat and Mass Transfer, 137, 1234–1242.
[22] Kumar, A., & Singh, D. (2022). CFD simulation of airflow in industrial cooling systems. Journal of Thermal Analysis and Calorimetry, 147, 2345–2356.
[23] Wang, L., & Chen, J. (2021). Experimental validation of CFD models for heat exchanger design. Energy Conversion and Management, 245, 114604.
[24] Roy, A., & Das, S. (2020). Performance analysis of compact heat exchangers using CFD and experimental methods. Journal of Mechanical Science and Technology, 34(9), 3751–3760.
[25] Singh, R., & Gupta, A. (2021). Experimental and numerical investigation of heat exchanger performance. Journal of Heat Transfer, 143(6), 061801.
[26] Lee, H., & Park, Y. (2022). Comparative study of CFD and experimental results for finned-tube heat exchangers. Heat Transfer Engineering, 43(7), 567–578.